

# Enhancing Data-based Fault Isolation Through Nonlinear Control: Application to a Polyethylene Reactor

Benjamin J. Ohran, David Muñoz de la Peña, Panagiotis D. Christofides and James F. Davis

**Abstract**—The present work proposes a method for data-based fault diagnosis that takes into account the design of the feedback control law in order to perform fault detection and isolation. This method allows isolating certain faults in a specifically structured closed-loop system using only a data-based approach. This is achieved through the design of appropriate nonlinear control laws that allow isolating given faults by effectively decoupling the dependency between certain process state variables. The theoretical results are demonstrated through a gas-phase polyethylene reactor example.

## I. INTRODUCTION

Handling process and control system failures efficiently is an issue of increasing importance in the context of chemical process control. Automation tends to increase the vulnerability of the plant to faults which can potentially cause a host of undesired economic, environmental and safety problems. One way of reducing the risk of such problems is through fault-tolerant control. Fault-tolerant control has been an active area of research over the past ten years and has motivated many research studies within the context of aerospace engineering [1], [2], [3]. Methods of fault-tolerant control utilize system redundancy to reconfigure a faulty control scheme to one that does not rely upon the failed process or equipment. In order to perform fault-tolerant control it is necessary to quickly detect the presence of a fault and isolate the unit or process in which the failure has occurred. Thus, early and accurate fault detection and isolation (FDI) may allow corrective action to avoid problems during a failure (see, for example, [4], [5]).

The proposed FDI method combines data-based fault detection methods with model-based controller design techniques to perform fault isolation. Detection is based exclusively on process measurements while isolation relies on a specifically enforced structure in the closed-loop system. Generally, data-based methods analyze measured data to give a picture of the location and trajectory of the system in the state-space. Historical process data from faulty operation can then be compared to the current operating data to diagnose a given fault [6], [7]. Data-based methods have

been developed that process the measured data to reduce the dimensions and extract information about the data under common-cause variation using principle component analysis (PCA) or partial least squares (PLS) [6]. Methods that use this reduced PCA space and consequent null space to gain further insight into the process include techniques such as contribution plots [8], multiblock PCA [9] and multiscale PCA [10]. For a comprehensive review of data-based fault detection and isolation methods, the reader may refer to [11]. One of the main drawbacks of currently available data-based methods is that they commonly require fault-specific historical data that may be costly to obtain. Additionally, due to the nonlinear nature of chemical processes, it is often difficult to distinguish regions of faulty operation due to overlap. In general, most data-based FDI methods are based on the premise that the controller is designed independently of the possible faults that might occur and design the fault detection and isolation scheme based on the closed-loop system.

Motivated by these issues, a data-based fault detection and isolation scheme is proposed that is able to isolate a given set of faults if the closed-loop system satisfies certain isolability conditions. We explicitly characterize this set of isolability conditions and show that it is possible, under certain conditions, to design a feedback control law that guarantees that the origin of the closed-loop system is asymptotically stable and that it satisfies these conditions. In this way, the design of the controller is introduced into the FDI strategy. This is achieved through the use of appropriate nonlinear control laws that allow isolating given faults by effectively decoupling the dependency between certain process state variables. In a previous work [12], feedback linearization was used to achieve the desired closed-loop structure. In the present work, this result is generalized to a broader family of controllers and is demonstrated through an application to a gas-phase polyethylene reactor.

## II. SYSTEM MODEL

This work focuses on nonlinear systems subject to faults with the following state-space description

$$\dot{x} = f(x, u, d) \quad (1)$$

where  $x \in \mathbb{R}^n$  denotes the vector of state variables,  $u \in \mathbb{R}^m$  denotes the vector of input variables and  $d \in \mathbb{R}^p$  denotes the vector of  $p$  possible faults. Normal operating conditions are defined by  $d = 0$ . Each component  $d_k, k = 1, \dots, p$  of vector  $d$  characterizes the occurrence of a given fault. When fault  $k$  occurs, variable  $d_k$  can take any value. The system of

Financial support from NSF, CTS-0529295, is gratefully acknowledged. Benjamin J. Ohran, Panagiotis D. Christofides and James F. Davis are with the Department of Chemical and Biomolecular Engineering, University of California, Los Angeles, CA 90095-1592, USA. Panagiotis D. Christofides is also with the Department of Electrical Engineering, University of California, Los Angeles, CA 90095-1592, USA. David Muñoz de la Peña is with the Departamento de Ingeniería de Sistemas y Automática, Universidad de Sevilla, Camino de los Descubrimientos S/N, Sevilla 410092, Spain, ohran@ucla.edu, davidmps@cartuja.us.es, pdc@seas.ucla.edu, jdavis@conet.ucla.edu.

Eq.1 under normal operating conditions and zero input has an equilibrium point at the origin, that is,  $f(0, 0, 0) = 0$ .

Before proceeding with the theoretical development, it is important to state that the proposed FDI method brings together model-based analysis and controller design techniques for nonlinear, deterministic ordinary differential equation systems and statistical data-based fault-diagnosis techniques. These will be applied to the closed-loop system to diagnose faults that affect the process outside of the region determined by the common-cause process variation. To this end, we will first state the isolability conditions for the closed-loop system that need to be enforced by the appropriate control laws on the basis of the nonlinear deterministic system of Eq.1. Subsequently, we will introduce additive autocorrelated noise in the right-hand side of Eq.1 and additive Gaussian noise in the measurements of the vector  $x$  to compute the region of operation of the process variable,  $x$ , under common-cause variance. Finally, we will demonstrate that the enforcement of an isolable structure in the closed-loop system by an appropriate feedback law allows isolating specific faults whose effect on the closed-loop system leads to sustained process operation outside of the region of common-cause variance.

Under the assumption of single-fault occurrence, we propose a novel data-based fault detection and isolation technique based on the structure of the closed-loop system. We provide the conditions under which this technique can be applied and show that for certain systems, the controller can be designed to guarantee that these conditions are satisfied as well as to stabilize the closed-loop. The main objective is to design a state feedback controller  $u(x)$  such that the origin of the system of Eq.1 in closed-loop with this controller is asymptotically stable under normal operating conditions and the closed-loop system satisfies the isolability conditions needed to apply the proposed FDI method. In order to present the FDI method, we need to define the incidence graph of a system and its reduced representation. The following definitions are motivated by standard results in graph theory [13]. This kind of graph analysis has been applied before in the context of control, see for example [14].

*Definition 1:* The incidence graph of an autonomous system  $\dot{x} = f(x)$  with  $x \in \mathbb{R}^n$  is a directed graph defined by  $n$  nodes, one for each state,  $x_i$ , of the system. A directed arc with origin in node  $x_i$  and destination in node  $x_j$  exists if and only if  $\frac{\partial f_j}{\partial x_i} \neq 0$ .

The incidence graph of a system shows the dependence of the time derivatives of its states. Figure 1 shows the incidence graph of the following system:

$$\begin{aligned} \dot{x}_1 &= -2x_1 + x_2 + d_1 \\ \dot{x}_2 &= -2x_2 + x_1 + d_2 \\ \dot{x}_3 &= -2x_3 + x_1 + d_3 \end{aligned} \quad (2)$$

when  $d_1 = d_2 = d_3 \equiv 0$ . A path from node  $x_i$  to node  $x_j$  is a sequence of connected arcs that starts at  $x_i$  and reaches  $x_j$ . A path through more than one arc that starts and ends at the same node is denoted as a loop. States that belong to a loop have mutually dependent dynamics, and any

disturbance affecting one of them also affects the trajectories of the rest. The mutual dependence of the dynamics of the states that belong to a given loop makes data-based isolation of faults that affect the system a difficult task. The following definition introduces the reduced incidence graph of an autonomous system. In this graph, the nodes of the incidence graph belonging to a given loop are united in a single node. This allows identifying which states do not have mutually dependant dynamics.

*Definition 2:* The reduced incidence graph of an autonomous system  $\dot{x} = f(x)$  with  $x \in \mathbb{R}^n$  is the directed graph of nodes  $q_i$ , where  $i = 1, \dots, N$ , that has the maximum number of nodes,  $N$ , and satisfies the following conditions:

- To each node  $q_i$  there corresponds a set of states  $X_i = \{x_j\}$ . These sets of states are a partition of the state vector of the system, i.e.,

$$\bigcup X_i = \{x_1, \dots, x_n\}, \quad X_i \cap X_j = \emptyset, \quad \forall i \neq j.$$

- A directed arc with origin  $q_i$  and destination  $q_j$  exists if and only if  $\frac{\partial f_l}{\partial x_k} \neq 0$  for some  $x_l \in X_i$ ,  $x_k \in X_j$ .
- There are no loops in the graph.

In the reduced incidence graph, states that belong to a loop in the incidence graph correspond to a single node. In this way, the states of the system are divided into subsystems that do not have mutually dependent dynamics; that is, there are no loops connecting them. The arcs of the graph indicate that there exists a state corresponding to the origin node that affects a state corresponding to the destination node. Note that the reduced incidence graph can be always obtained, but for strongly coupled systems, it may be defined by a single node.

In the incidence graph of the system of Eq.2 there is a loop that contains states  $x_1$  and  $x_2$ . The reduced incidence graph of the system of Eq.2 contains two nodes. Node  $q_1$  corresponds to the states of the loop, that is,  $X_1 = \{x_1, x_2\}$ . Node  $q_2$  corresponds to  $X_2 = x_3$ . Figure 1 shows the reduced incidence graph of the system of Eq.2. It can be seen that in the reduced incidence graph there are no loops.

In the following section, we introduce the notion of the signature of a fault, or the set of states whose trajectories are affected by a fault and propose an FDI scheme based on this notion.

### III. SIGNATURE OF A FAULT

In this section, we introduce the set of conditions under which it is possible to isolate a fault using only state measurements. To this end, we define the isolability graph of an autonomous system.

*Definition 3:* The isolability graph of an autonomous system  $\dot{x} = f(x, d)$  with  $x \in \mathbb{R}^n$ ,  $d \in \mathbb{R}^p$  is a directed graph made of the  $N$  nodes of the reduced incidence graph of the system  $\dot{x} = f(x, 0)$  and  $p$  additional nodes, one for each possible fault  $d_k$ . The graph contains all the arcs of the reduced incidence graph of the system  $\dot{x} = f(x, 0)$ . In addition, a directed arc with origin in fault node  $d_k$  and destination to a state node  $q_j$  exists if and only if  $\frac{\partial f_l}{\partial d_k} \neq 0$  for some  $x_l \in X_j$ .

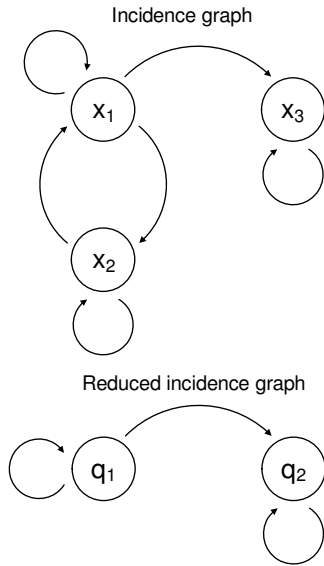


Fig. 1. Incidence graph and reduced incidence graph of the system of Eq.2.

Figure 2 shows the isolability graph of the system of Eq.2. The isolability graph of an autonomous system subject to  $p$  faults shows, in addition to the incidence arcs of the reduced incidence graph, which loops of the system are affected by each possible fault. Based on this graph we can define the signature of a fault.

**Definition 4:** The signature of a fault  $d_k$  of an autonomous system subject to  $p$  faults  $\dot{x} = f(x, d)$  with  $x \in \mathbb{R}^n$ ,  $d \in \mathbb{R}^p$  is a binary vector  $W^k$  of dimension  $N$ , where  $N$  is the number of nodes of the reduced incidence graph of the system. The  $i^{th}$  component of  $W^k$ , denoted  $W_i^k$ , is equal to one if there exists a path in the isolability graph from the node corresponding to fault  $k$  to the node  $q_i$  corresponding to the set of states  $X_i$ , or zero otherwise.

The signature of a fault indicates the set of states that are affected by the fault. If each of the corresponding signatures of the faults is different, then it is possible to isolate the faults using a data-based fault-detection method. Faults  $d_1$  and  $d_2$  in the system of Eq.2 have the same signature,  $W^1 = [1 \ 1]^T$ , because  $d_1$  and  $d_2$  both directly affect  $q_1$  and there is a path from  $q_1$  to  $q_2$ . This implies that both faults affect the same states and upon detection of a fault with the signature  $W^1 = [1 \ 1]^T$ , it is not possible to distinguish between them based upon the signature. On the other hand, the signature of fault  $d_3$  in the same system is  $W^1 = [0 \ 1]^T$  because there is no path to  $q_1$  from  $q_2$ , which is the node directly affected by  $d_3$ . This implies that the states corresponding to node  $q_1$  are effectively decoupled from fault  $d_3$ . This allows distinguishing between a fault in  $d_3$  and a fault in either  $d_1$  or  $d_2$  in the system of Eq.2 based on the profiles of the state trajectories.

#### IV. DATA-BASED ISOLATION

Data-based methods for fault detection in multivariate systems are well established in statistical process control.

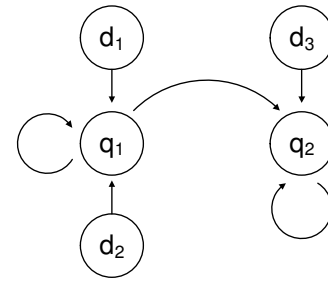


Fig. 2. Isolability graph of the system of Eq.2.

A common approach to monitoring multivariate process performance is based upon Hotelling's  $T^2$  statistic, which allows multivariate processes to be monitored using a single statistic with a well-defined threshold for normal operation. A generalization of Student's t-statistic, Hotelling's method found in [15] normally calls for random samples consisting of multiple observations per sample. The covariance matrix is then calculated from the observations in each sample (see also [16]). This method has been adapted to use single observations in order to be more compatible with the nature of continuous chemical process systems [16], [17]. In another work [18], both approaches were considered; however, the present work uses only the method of single observations in the application example of Section VI.

Given a multivariate state vector  $x$  of dimension  $n$ , the  $T^2$  statistic can be computed using the mean  $\bar{x}$  and the estimated covariance matrix  $S$  of process data obtained under normal operating conditions (see, for example, [6], [8]).

$$T^2 = (x - \bar{x})^T S^{-1} (x - \bar{x}). \quad (3)$$

The upper control limit for the  $T^2$  statistic can be calculated from its distribution, with on the assumption that the data are multivariate normal, according to the following formula:

$$T_{UCL}^2 = \frac{(h^2 - 1)n}{h(h - n)} F_{\alpha}(n, h - n) \quad (4)$$

where  $h$  is the number of historical measurements used in approximating  $S$ ,  $F_{\alpha}(n, h - n)$  is the value on the  $F$  distribution with  $(n, h - n)$  degrees of freedom for which there is probability  $\alpha$  of a greater or equal value occurring. Thus  $\alpha$  is the probability of a Type I error or false alarm. Because  $T^2$  is a positive quantity, the test has no lower bound. Note that the requirement of multivariate normal data is generally a reasonable assumption since data that may be serially correlated in open-loop operation is frequently more normal under feedback control on a large timescale [16].

We propose to monitor the following statistics based on the state trajectories of the system of Eq.1 in closed-loop with a given feedback controller  $u(x)$ :

- $T^2$  statistic based on the full state  $x$  with upper control limit  $T_{UCL}^2$ .
- $T_i^2$  statistic with  $i = 1, \dots, N$  based on the states  $x_j \in X_i$ , where  $X_i$  are the sets of states corresponding to each one of the nodes of the reduced incidence graph.

To each  $T_i^2$  statistic a corresponding upper control limit  $T_{UCLi}^2$  is assigned.

The fault detection and isolation procedure then follows the steps given below:

1. A fault is detected if  $T^2(t) > T_{UCL}^2 \forall t, t_f \leq t \leq T_P$  where  $T_P$  is chosen so that the window  $T_P - t_f$  is large enough to allow fault isolation within a desired degree of confidence and depends on the process time constants and potentially on available historical information of the process behavior.
2. A fault that is detected can be isolated if the signature vector of the fault  $W(t_f, T_P)$  can be built as follows:

$$T_i^2(t) > T_{UCLi}^2 \forall t, t_f \leq t \leq T_P \rightarrow W_i(t_f, T_P) = 1.$$

$$T_i^2(t) \not> T_{UCLi}^2 \forall t, t_f \leq t \leq T_P \rightarrow W_i(t_f, T_P) = 0.$$

In such a case, fault  $d_k$  is detected at time  $T_P$  if  $W(t_f, T_P) = W^k$ . If two or more faults are defined by the same signature, isolation between them is not possible on the basis of the fault signature obtained from the isolability graph.

This FDI scheme can be applied if the signatures of the closed-loop system faults are different. Note that the signature of a fault depends on the structure of the closed-loop system, in particular, on the isolability graph. For example, if the reduced incidence graph has only one node, isolation is not possible. In the following section, we propose to design the feedback controller  $u(x)$  to guarantee that the closed-loop reduced incidence graph has more than one node, that there exist faults with different signatures and that the origin of the closed-loop system is asymptotically stable.

*Remark 1:* The upper control limit is chosen taking into consideration common-cause variance, including process and sensor noise, in order to avoid false alarms. Thus, small disturbances or failures may go undetected if the magnitude and effect of the disturbance is similar to that of the inherent process variance. For this reason, a fault  $d_k$  must be sufficiently large in order for  $T_i^2(t)$  to exceed the threshold  $T_{UCLi}^2 \forall t, t_f \leq t \leq T_P$ . It is assumed that if a fault  $d_k$  is not large enough to cause  $T_i^2(t)$  to exceed the threshold  $T_{UCLi}^2 \forall t, t_f \leq t \leq T_P$  (where  $t_f$  is the time in which  $T_i^2(t_f) \geq T_{UCL}^2$  for the first time) then the fault is not sufficiently large and its effect on the closed-loop system, from the point of view of faulty behavior, is not of major consequence. Therefore, such a  $d_k$  is not considered to be a fault. However, it should be noted that a fault  $d_k$  that is large enough to cause the  $T^2$  derived from the full state vector,  $x$ , to cross the upper control limit signaling a fault may not be large enough to signal a fault in all of the affected subgroups. In this case, it is possible to have a false isolation.

## V. CONTROLLER ENHANCED ISOLATION

In general, control laws are designed without taking into account the FDI scheme of the control system. In this section, we propose to design an appropriate nonlinear control law to allow isolation of given faults using the method proposed in the previous section by effectively decoupling

TABLE I  
NOISE PARAMETERS

	$\sigma_p$	$\sigma_M$	$\phi$
$[In]$	1E-3	5E-2	0
$[M_1]$	1E-3	5E-2	0.7
$Y$	1E-3	1E-2	0.7
$T$	5E-3	5E-2	0.7
$T_{g1}$	5E-3	5E-2	0.7
$T_{w1}$	5E-3	5E-2	0.7

the dependency between certain process state variables. The purpose is to obtain a reduced incidence graph of the closed-loop system which provides different signatures for different faults. The achievement of the key requirement, which is the enforcement of a specific structure in the closed-loop system, can be accomplished by a variety of nonlinear control laws. In a previous paper [12], we utilized feedback linearization to achieve this task. In the present work, however, we show that other control strategies can be applied. In particular we provide a controller that can be applied to nonlinear systems with the following state space description:

$$\begin{aligned} \dot{x}_1 &= f_{11}(x_1) + f_{12}(x_1, x_2) + g_1(x_1, x_2)u + d_1 \\ \dot{x}_2 &= f_2(x_1, x_2) + d_2. \end{aligned}$$

With a state feedback controller of the form:

$$u(x_1, x_2) = -\frac{f_{12}(x_1, x_2) - v}{g_1(x_1, x_2)}$$

the closed-loop system takes the form

$$\begin{aligned} \dot{x}_1 &= f_{11}(x_1) + v(x_1) + d_1 \\ \dot{x}_2 &= f_2(x_1, x_2) + d_2 \end{aligned}$$

where  $v(x_1)$  has to be designed in order to achieve asymptotic stability of the origin for  $x_1$  when  $d_1 = 0$ . Note that stabilizing control laws that provide explicitly-defined regions of attraction for the closed-loop system have been developed using Lyapunov techniques for specific classes of nonlinear systems, particularly input-affine nonlinear systems; the reader may refer to [19], [20] for results in this area. The origin of the closed-loop system is asymptotically stable if  $x_2 = f_{22}(x_1, x_2)$  is input-to-state stable with respect to  $x_1$  for  $d_2 = 0$ . In this case the proposed controller guarantees stability of the closed-loop system, as well as different signatures for faults  $d_1$  and  $d_2$ . Note that the reduced incidence graph is defined by two nodes corresponding to both states and the signatures are given by  $W^1 = [1 \ 1]^T$ ,  $W^2 = [0 \ 1]^T$ .

## VI. APPLICATION TO A POLYETHYLENE REACTOR

The method of controller enhanced isolation will be demonstrated using a model of an industrial gas phase polyethylene reactor. The feed to the reactor is made up of ethylene, comonomer, hydrogen, inerts, and catalyst. A recycle stream of unreacted gases flows from the top of the reactor and is cooled by passing through a water-cooled heat exchanger. Cooling rates in the heat exchanger are adjusted by mixing cold and warm water streams while maintaining a constant total cooling water flowrate through the heat

exchanger. Mass balances on hydrogen and comonomer have not been considered in this study because hydrogen and comonomer have only mild effects on the reactor dynamics [21]. A mathematical model for this reactor has the form:

$$\begin{aligned}
\frac{d[In]}{dt} &= \frac{1}{V_g}(F_{In} - \frac{[In]}{[M_1] + [In]}b_t) \\
\frac{d[M_1]}{dt} &= \frac{1}{V_g}(F_{M_1} - \frac{[M_1]}{[M_1] + [In]}b_t - R_{M_1}) \\
\frac{dY_1}{dt} &= F_c a_c - k_{d_1} Y_1 - \frac{R_{M_1} M_{W_1} Y_1}{B_w} + d_2 \\
\frac{dY_2}{dt} &= F_c a_c - k_{d_2} Y_2 - \frac{R_{M_1} M_{W_1} Y_2}{B_w} + d_2 \\
\frac{dT}{dt} &= \frac{H_f + H_{g1} - H_{g0} - H_r - H_{pol}}{M_r C_{pr} + B_w C_{ppol}} + d_1 \\
\frac{dT_{w_1}}{dt} &= \frac{F_w}{M_w}(T_{wi} - T_{w_1}) - \frac{UA}{M_w C_{pw}}(T_{w_1} - T_{g_1}) \\
\frac{dT_{g_1}}{dt} &= \frac{F_g}{M_g}(T - T_{g_1}) + \frac{UA}{M_g C_{pg}}(T_{w_1} - T_{g_1}) + d_3
\end{aligned} \tag{5}$$

where

$$\begin{aligned}
b_t &= V_p C_v \sqrt{([M_1] + [In])RRT - P_v} \\
R_{M_1} &= [M_1] k_{p0} e^{\frac{-E_a}{R}(\frac{1}{T} - \frac{1}{T_f})} (Y_1 + Y_2) \\
C_{pg} &= \frac{[M_1]}{[M_1] + [In]} C_{pm1} + \frac{[In]}{[M_1] + [In]} C_{pIn} \\
H_f &= (F_{M_1} C_{pm1} + F_{In} C_{pIn})(T_{feed} - T_f) \\
H_{g1} &= F_g (T_{g_1} - T_f) C_{pg} \\
H_{g0} &= (F_g + b_t)(T - T_f) C_{pg} \\
H_r &= H_{reac} M_{W_1} R_{M_1} \\
H_{pol} &= C_{ppol}(T - T_f) R_{M_1} M_{W_1}
\end{aligned} \tag{6}$$

The definitions for all the variables used in Eqs.5-6 are given in Table II and their values can be found in [22] (see also [23]). Under normal operating conditions, the open-loop system behaves in an oscillatory fashion (i.e., the system possesses an open-loop unstable steady-state surrounded by a stable limit cycle). The open-loop unstable steady-state around which the system will be controlled is

$$\begin{aligned}
[In]_{ss} &= 439.7 \frac{mol}{m^3} & [M_1]_{ss} &= 326.7 \frac{mol}{m^3} \\
Y_{1ss}, Y_{2ss} &= 3.835 mol & T_{ss} &= 356.2 K \\
T_{g1ss} &= 290.4 K & T_{w1ss} &= 294.4 K
\end{aligned}$$

Note that with the given parameters, the dynamics of  $Y_1, Y_2$  are identical and will be reported in the results section as a single combined state. In this example, we consider three possible faults,  $d_1, d_2$ , and  $d_3$  which represent a change in the feed temperature, catalyst deactivation and a change in the recycle gas flow rate, respectively. The manipulated inputs are the feed temperature,  $T_{feed}$ , and the inlet flow rate of ethylene,  $F_{M_1}$ .

The control objective is to stabilize the system at the open-loop unstable steady state. In addition, in order to apply the proposed FDI scheme, the controller must guarantee that the closed-loop system satisfies the isolability conditions. The open-loop system is highly coupled. If the controller does not impose a specific structure, all the states have mutually dependent dynamics (i.e., they consist of one node in the isolability graph). In the present work, we propose to design a nonlinear controller to decouple  $[In]$ ,  $[M_1]$  and  $T$  from  $(Y_1, Y_2)$  and from  $T_{w_1}$  and  $T_{g_1}$ . In this way, the resulting closed-loop system consists of three subsystems (i.e., three nodes in the isolability graph) that do not have mutually dependent dynamics. In addition, the signature of each of the three faults is different, and thus, the fault isolability conditions are satisfied. In order to accomplish this objective, we define the following control laws:

$$\begin{aligned}
F_{M_1} &= u_2 V_g + F_{M_1ss} \\
T_{feed} &= \frac{u_1 (M_r C_{pr} + B_w C_{ppol}) + H_{fss}}{F_{M_1} C_{pm1} + F_{In} C_{pIn}} + T_f
\end{aligned} \tag{7}$$

with

$$\begin{aligned}
u_1 &= \frac{H_r - H_{rss} + H_{pol} - H_{polss} - H_{g1} + H_{g1ss}}{M_r C_{pr} + B_w C_{ppol}} + v_1 \\
u_2 &= \frac{R_{M_1} - R_{M_1ss}}{V_g} + v_2
\end{aligned} \tag{8}$$

where terms with the subscript  $ss$  are constants evaluated at the steady state and  $v_1, v_2$  are external inputs that will allow us to stabilize the resulting closed-loop system. The dynamics of the affected states,  $T$  and  $[M_1]$ , take the following form in the closed-loop system:

$$\begin{aligned}
\frac{d[M_1]}{dt} &= [F_{M_1} - \frac{[M_1]}{[M_1] + [In]}b_t - R_{M_1ss}] \frac{1}{V_g} + v_2 \\
\frac{dT}{dt} &= \frac{H_f + H_{g1ss} - H_{g0} - H_{rss} - H_{polss}}{M_r C_{pr} + B_w C_{ppol}} + v_1 + d_1
\end{aligned} \tag{9}$$

It can be seen that these states only depend on  $[In]$ ,  $[M_1]$  and  $T$ . The closed-loop system under the control law defined in Eq.7 has a reduced incidence graph with three nodes  $q_1, q_2$  and  $q_3$  corresponding to the three partially decoupled subsystems  $X_1 = \{[In], [M_1], T\}$ ,  $X_2 = \{Y_1, Y_2\}$  and  $X_3 = \{T_{g_1}, T_{w_1}\}$ , respectively. The resulting isolability graph for the closed-loop system is shown in Figure 3. This structure leads to each of the three faults  $d_1, d_2$  and  $d_3$  having unique signatures  $W^1 = [1 \ 1 \ 1]^T$ ,  $W^2 = [0 \ 1 \ 0]^T$  and  $W^3 = [0 \ 0 \ 1]^T$  and allows fault detection and isolation in the closed-loop system using the proposed data-based FDI scheme.

In order to study the stability properties of the closed-loop system, we study the stability of the equilibrium point for each subsystem assuming that the rest of the states are at the equilibrium point. It can be seen that both subsystems  $X_2 = \{Y_1, Y_2\}$  and  $X_3 = \{T_{g_1}, T_{w_1}\}$  are stable. This

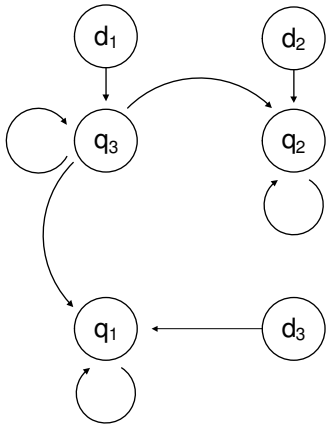


Fig. 3. Isolability graph for the system of Eq.5.

implies that to obtain a stable closed-loop system, the control inputs  $v_1, v_2$  have to be designed to stabilize subsystem  $X_1 = \{[In], [M_1], T\}$ . In the present example, we use two PI controllers that regulate each state independently. By extensive simulations, the PI controllers have been tuned to stabilize the equilibrium of the closed-loop system and achieve a desired closed-loop response. It is important to remark that for the purpose of this example, any controller that stabilizes subsystem  $X_1$  can be used, as the main objective is to demonstrate the data-based FDI scheme proposed. The PI controllers are defined as follows:

$$\begin{aligned} v_1(t) &= K_1(T_{ss} - T + \frac{1}{\tau_1} \int_{t_0}^t (T_{ss} - T)dt) \\ v_2(t) &= K_2([M_1]_{ss} - [M_1] + \frac{1}{\tau_2} \int_{t_0}^t ([M_1]_{ss} - [M_1])dt) \end{aligned} \quad (10)$$

with  $K_1 = 0.005$ ,  $K_1 = 0.0075$ ,  $\tau_2 = 1000$ ,  $\tau_1 = 500$ . We will refer to the controller defined by Eqs.7, 8 and 10 as the “decoupling” controller. Additionally, for comparison purposes, a controller is used that stabilizes the closed-loop system, but does not take into account the isolability conditions of the proposed FDI method. Specifically, two PI controllers will be used to regulate  $T$  and  $M_1$ . This will be denoted as the “PI-only” control law. The inputs  $F_{M1}$  and  $T_{feed}$  are defined by Eq.7, but in this case,  $u_1$  and  $u_2$  are evaluated by applying the PI controllers of Eq.10 with the same tuning parameters to the states  $T$  and  $M_1$ . The PI-only controller stabilizes the equilibrium point under normal operating conditions, however, all the states are mutually dependent, or in other words the reduced incidence graph consists of only one node. This implies that every fault affects all the state trajectories, making isolation of the fault a difficult task. The proposed FDI scheme cannot be applied because the closed-loop does not satisfy the isolability conditions, i.e., all the system faults have the same signature.

Simulations have been carried out for several scenarios to demonstrate the effectiveness of the proposed FDI scheme in detecting and isolating the three faults  $d_1$ ,  $d_2$ , and  $d_3$ . In all the simulations, sensor measurement and process noise

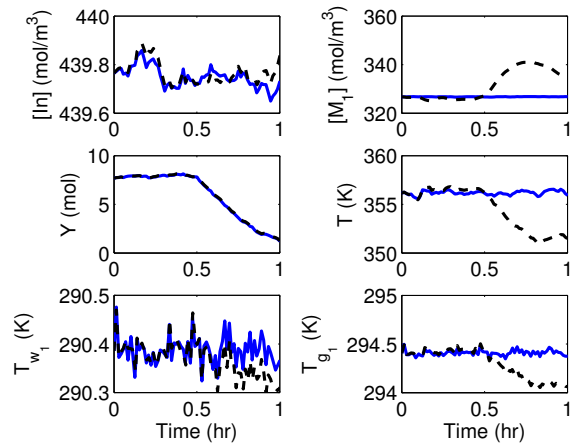


Fig. 4. State trajectories of the closed-loop system under the decoupling (solid) and PI-only (dashed) controllers with a fault  $d_2$  at  $t = 0.5hr$ .

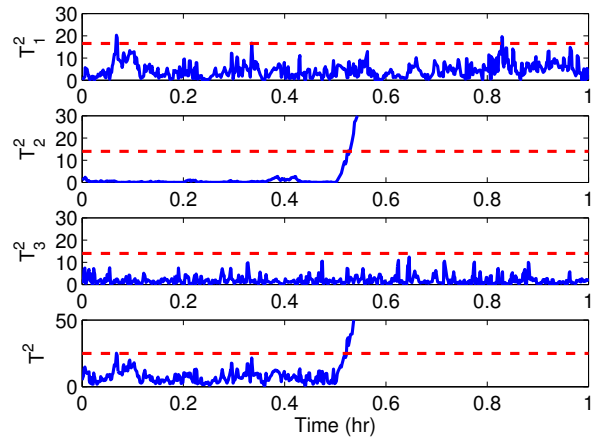


Fig. 5. Statistics  $T^2$ ,  $T_1^2$ ,  $T_2^2$ , and  $T_3^2$  of the closed-loop system under the decoupling controller with a failure in  $d_2$  at  $t = 0.5hr$ .

were included. The sensor measurement noise trajectory was generated using a sample time of ten seconds and a zero-mean normal distribution with standard deviation  $\sigma_M$ . The autoregressive process noise was generated discretely as  $w_k = \phi w_{k-1} + \xi_k$  where  $k = 0, 1, \dots$  is the discrete time step, with a sample time of ten seconds where  $\phi$  is the autoregressive coefficient and  $\xi_k$  is obtained at each sampling step using a zero-mean normal distribution with standard deviation  $\sigma_p$ . Sensor measurement and process noise are evaluated independently for each state variable. The process and sensor noise for  $Y_1$  and  $Y_2$  are assumed to be equal. Table I provides the values of the noise parameters for each state of the system of Eq. 5. A window of ten minutes was used for detecting faults (i.e.,  $T_P - t_f = 10min$ ). Although the states in the polyethylene system are serially correlated on a short timescale, this is compensated for by using a large amount of historical data for estimating  $S$ . This, along with the fact that feedback control makes the closed-loop system more normally distributed (see [16]), means that the multivariate normal assumption necessary for applying the single observation  $T^2$  statistic is reasonable. Figure 6 shows

TABLE II

POLYETHYLENE REACTOR EXAMPLE PROCESS VARIABLES.

$a_c$	active site concentration of catalyst
$b_t$	overhead gas bleed
$B_w$	mass of polymer in the fluidized bed
$C_{pm1}$	specific heat capacity of ethylene
$C_v$	vent flow coefficient
$C_{pw}, C_{pIn}, C_{ppol}$	specific heat capacity of water, inert gas and polymer
$E_a$	activation energy
$F_c, F_g$	flow rate of catalyst and recycle gas
$F_{In}, F_{M_1}, F_w$	flow rate of inert, ethylene and cooling water
$H_f, H_{g0}$	enthalpy of fresh feed stream, total gas outflow stream from reactor
$H_{g1}$	enthalpy of cooled recycle gas stream to reactor
$H_{pol}$	enthalpy of polymer
$H_r$	heat liberated by polymerization reaction
$H_{reac}$	heat of reaction
$[In]$	molar concentration of inerts in the gas phase
$k_{d1}, k_{d2}$	deactivation rate constant for catalyst site 1, 2
$k_{p0}$	pre-exponential factor for polymer propagation rate
$[M_1]$	molar concentration of ethylene in the gas phase
$M_g$	mass holdup of gas stream in heat exchanger
$M_r C_{pr}$	product of mass and heat capacity of reactor walls
$M_w$	mass holdup of cooling water in heat exchanger
$M_{W1}$	molecular weight of monomer
$P_v$	pressure downstream of bleed vent
$R, RR$	ideal gas constant, unit of $\frac{J}{mol \cdot K}, \frac{m^3 \cdot atm}{mol \cdot K}$
$T, T_f, T_{feed}$	reactor, reference, feed temperature
$T_{g1}, T_{w1}$	temperature of recycle gas, cooling water stream from exchanger
$T_{wi}$	inlet cooling water temperature to heat exchanger
$UA$	product of heat exchanger coefficient with area
$V_g$	volume of gas phase in the reactor
$V_p$	bleed stream valve position
$Y_1, Y_2$	moles of active site type 1, 2

that the distribution of the state measurements over a long period of fault-free operation is approximately Gaussian.

For each failure  $d_k$ , two simulations have been carried out. One using the decoupling controller and another using the PI-only controller. Both simulations have been arrived at using the same sensor measurement and process noise trajectories. The three different failures with values  $d_1 = 10 \frac{K}{s}$ ,  $d_2 = -0.002 \frac{mol}{s}$ , and  $d_3 = 300 \frac{K}{s}$  were introduced at time  $t = 0.5hr$ . Figure 4 shows the state trajectories of the closed-loop system under the decoupling controller (solid line) and the PI-only controller (dashed line) for the system with a fault in  $d_2$ . It can be seen that for the PI-only controller, each time a fault occurs, all states deviate from the equilibrium point. This makes isolation a difficult task. However, the closed-loop state trajectories under the decoupling controller show that when a given fault occurs, not all state trajectories are affected. The decoupling of some states from given faults

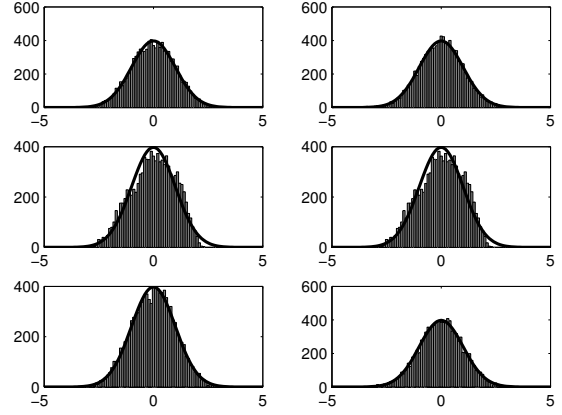


Fig. 6. Polyethylene reactor example. Distribution of normalized, fault-free operating data compared with a normal distribution of the same mean and covariance.

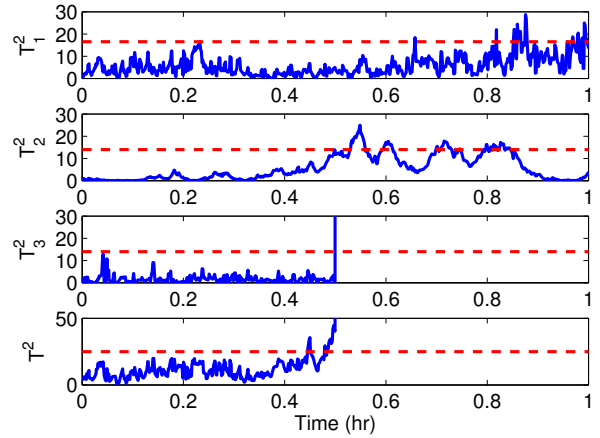


Fig. 7. Statistics  $T^2$ ,  $T_1^2$ ,  $T_2^2$ , and  $T_3^2$  of the closed-loop system under the decoupling controller with a failure in  $d_3$  at  $t = 0.5hr$ .

allow us to isolate the faults based on the  $T_i^2$  statistics.

The state trajectories of the closed-loop system under the decoupling controller were monitored using the  $T^2$  statistic based on all the states of the system of Eq. 5 and the  $T_i^2$  statistic corresponding to each one of the three subsystems  $X_1$ ,  $X_2$ ,  $X_3$ . Figures 5, 7 and 8 show the trajectories of  $T^2$ ,  $T_1^2$ ,  $T_2^2$  and  $T_3^2$  for each fault along with the corresponding upper control limits. Based on the fault detection and isolation procedure laid out in Section IV, each failure is defined by a unique signature that can be isolated based on the monitored statistics. Figure 5 shows the statistics corresponding to the simulation with a failure in  $d_2$ . The signature of  $d_2$  is  $W^2 = [0 \ 1 \ 0]^T$ , because the dynamics of the states corresponding to  $X_1$  and  $X_3$  are not affected by fault  $d_2$ ; that is, there is no path from the node corresponding to  $d_2$  to the nodes corresponding to  $X_1$  and  $X_2$  in the isolability graph of the closed-loop system. Figure 5 clearly shows the fault occurring at time  $t = 0.5hr$  and the signature that is expected with only  $T_2^2$  violates the upper control limit.

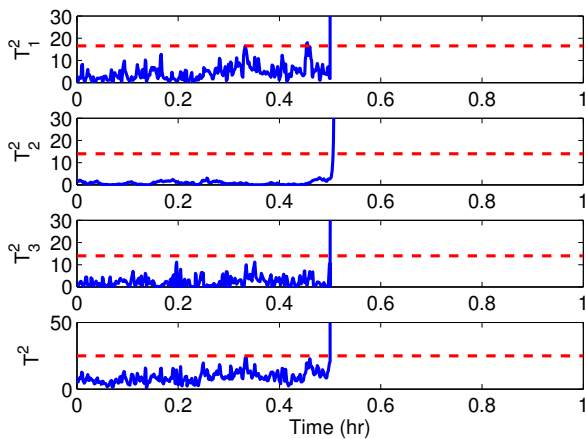


Fig. 8. Statistics  $T^2$ ,  $T_1^2$ ,  $T_2^2$ , and  $T_3^2$  of the closed-loop system under the decoupling controller with a failure in  $d_1$  at  $t = 0.5hr$ .

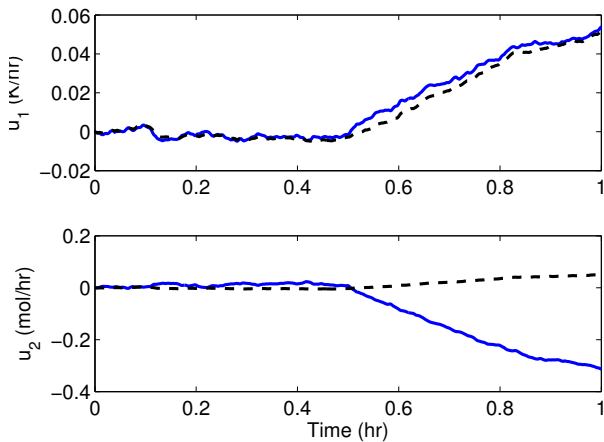


Fig. 9. Manipulated input values for both decoupling and PI-only control with a fault in  $d_2$  at  $t = 0.5hr$ .

The state trajectories of this faulty scenario of Figure 4 shows that there is a failure affecting  $Y$  starting at  $t = 0.5hr$ . The failure affects all the state trajectories under PI-only control but affects only  $Y$  for the system under decoupling control. Similarly, a failure in  $T_{g1}$  affects only subsystem  $X_3$ . The statistics in Figure 7 show that the signature of the fault is  $[0 \ 0 \ 1]^T = W^3$ . The signature of fault  $d_1$  is  $W^1 = [1 \ 1 \ 1]^T$ , meaning that this fault affects all the states in the closed-loop system. Figures 8 shows the corresponding statistics. Figure 9 shows the manipulated input trajectories for both controllers in the scenario with fault  $d_2$  occurring. It can be observed that the control action required under the decoupling control law is on the same order of magnitude as that of the PI-only controller and is not excessive relative to the normal demand under PI control.

## VII. CONCLUSIONS

This work has presented a general approach to integrating data-based fault detection with model-based controller design in a fault detection and isolation scheme. This approach

enforces a specific structure on the closed-loop system that facilitates fault isolation. This method was demonstrated using a polyethylene reactor example. By decoupling faults of interest from certain states, it was possible to achieve the required closed-loop structure to allow fault detection and isolation.

## REFERENCES

- [1] R. J. Patton, "Fault-tolerant control systems: The 1997 situation," in *Proceedings of the IFAC Symposium SAFEPROCESS 1997*, Hull, United Kingdom, 1997, pp. 1033–1054.
- [2] M. Blanke, R. Izadi-Zamanabadi, S. A. Bogh, and C. P. Lunau, "Fault-tolerant control systems – a holistic view," *Control Engineering Practice*, vol. 5, pp. 693–702, 1997.
- [3] D. H. Zhou and P. M. Frank, "Fault diagnostics and fault tolerant control," *IEEE Transactions on Aerospace and Electronic Systems*, vol. 34, pp. 420–427, 1998.
- [4] P. Mhaskar, A. Gani, N. H. El-Farra, C. McFall, P. D. Christofides, and J. F. Davis, "Integrated fault detection and fault-tolerant control of process systems," *AIChE Journal*, vol. 52, pp. 2129–2148, 2006.
- [5] P. Mhaskar, C. McFall, A. Gani, P. Christofides, and J. Davis, "Isolation and handling of actuator faults in nonlinear systems," *Automatica*, vol. 44, pp. 53–62, 2008.
- [6] J. Romagnoli and A. Palazoglu, *Introduction to Process Control*. CRC Press, 2006.
- [7] J. MacGregor and T. Kourti, "Statistical process control of multivariate processes," *Journal of Quality Technology*, vol. 28, pp. 409–428, 1996.
- [8] T. Kourti and J. MacGregor, "Multivariate SPC methods for process and product monitoring," *Journal of Quality Technology*, vol. 28, pp. 409–428, 1996.
- [9] J. A. Westerhuis, T. Kourti, and J. F. MacGregor, "Analysis of multiblock and hierarchical PCA and PLS models," *Journal of Chemometrics*, vol. 12, pp. 301–321, 1998.
- [10] B. R. Bakshi, "Multiscale PCA with application to multivariate statistical process monitoring," *AIChE Journal*, vol. 44, pp. 1596–1610, 1998.
- [11] V. Venkatasubramanian, R. Rengaswamy, S. Kavuri, and K. Yin, "A review of process fault detection and diagnosis part III: Process history based methods," *Computers and Chemical Engineering*, vol. 27, pp. 327–346, 2003.
- [12] B. J. Ofran, P. Mhaskar, D. Muñoz de la Peña, P. D. Christofides, and J. F. Davis, "Enhancing fault isolation through nonlinear controller design," in *Proceedings of 8th IFAC Symposium on Dynamics and Control of Process*, vol. 1, Cancun, Mexico, 2007, pp. 81–86.
- [13] F. Harary, *Graph Theory*. Perseus Books Publishing, 1969.
- [14] P. Daoutidis and C. Kravaris, "Structural evaluation of control configurations for multivariable nonlinear processes," *Chemical Engineering Science*, vol. 47, pp. 1091–1107, 1991.
- [15] H. Hotelling, "Multivariate quality control," in *Techniques of Statistical Analysis*, O. Eisenhart, Ed. McGraw-Hill, 1947, pp. 113–184.
- [16] D. C. Montgomery, *Introduction to statistical quality control*. John Wiley & Sons, 1996.
- [17] N. D. Tracy, J. C. Young, and R. L. Mason, "Multivariate control charts for individual observations," *Journal of Quality Technology*, vol. 24, pp. 88–95, 1992.
- [18] B. J. Ofran, D. Muñoz de la Peña, P. D. Christofides, and J. F. Davis, "Enhancing data-based fault isolation through nonlinear control," *AIChE Journal*, vol. 54, pp. 223–241, 2008.
- [19] P. Kokotovic and M. Arcak, "Constructive nonlinear control: a historical perspective," *Automatica*, no. 37, pp. 637–662, 2001.
- [20] P. D. Christofides and N. H. El-Farra, *Control of Nonlinear and Hybrid Process Systems: Designs for Uncertainty, Constraints and Time-Delays*. Berlin, Germany: Springer-Verlag, 2005.
- [21] K. B. McAuley, D. A. Macdonald, and P. J. McLellan, "Effects of operating conditions on stability of gas-phase polyethylene reactors," *AIChE Journal*, vol. 41, pp. 868–879, 1995.
- [22] S. A. Dadebo, M. L. Bell, P. J. McLellan, and K. B. McAuley, "Temperature control of industrial gas phase polyethylene reactors," *Journal of Process Control*, vol. 7, pp. 83–95, 1997.
- [23] A. Gani, P. Mhaskar, and P. D. Christofides, "Fault-tolerant control of a polyethylene reactor," *Journal of Process Control*, vol. 17, pp. 439–451, 2007.